Robotically-Assisted Titration Coupled to Ion Mobility-Mass Spectrometry Reveals the Interface Structures and Analysis Parameters Critical for Multiprotein Topology Mapping

*Yueyang Zhong, Jun Feng, and Brandon T. Ruotolo**

Department of Chemistry, University of Michigan, 930 N. University Ave., Ann Arbor, MI 48109

Supporting Information

X-ray and IM-MS Structure analysis. To quantitatively evaluate the agreement between X-ray and IM-MS structure information, we computed a number of values extracted from the CG models constructed from both datasets. Equation 1 defines the parameter R:

$$\mathbf{R} = \frac{Dim-Dim\,Distance}{Mon-Mon\,Distance} \quad (1)$$

which is a ratio of the distance between the geometric centers of the two dimeric subcomplexes that comprise the tetramer over the distance between the two monomeric units that comprise those dimers. We also computed the relative size differences between crystolographic and IM-measured monomers:

$$\%\ \mathbf{Monomer\ Size\ Difference} = \frac{(\frac{Mon_{Tet}})_{IM} - (\frac{Mon_{Tet}})_{Crystal}}{(\frac{Mon_{Tet}})_{Crystal}} \quad (2)$$

where the monomer size from both datasets is expressed as a fraction of the total complex size. A similar metric is also used in our data to evaluate dimer size agreement between X-ray and IM datasets:

$$\%\ \mathbf{Dimer\ Size\ Difference} = \frac{(\frac{Dim_{Tet}})_{IM} - (\frac{Dim_{Tet}})_{Crystal}}{(\frac{Dim_{Tet}})_{Crystal}} \quad (3)$$

For X-ray data analysis alone, we have developed several useful metrics that we use to evaluate the trends observed in our IM-MS dataset. First, we calculate the asphericity of protein subunits in complexes using Equation 4:

$$\mathbf{Monomer\ Asphericity\ Index} = \frac{L_{SD}}{L_{AV}} \quad (4)$$

where L_{AV} is the average distance between the protein center-of-mass and its surface, and L_{SD} is the standard deviation of all of the length measurements used to define L_{AV}. Larger index values indicate less-spherical monomers. The second method of X-ray structure analysis used here involves counting the number of inter-chain contacts within protein complexes. These values are normalized by the total molecular weight of the proteins studied here to generate a contact-per-unit mass (kDa) value for each tetramer included in this report. Cut-off distances for inter-protein contacts were defined as 4 Å for both salt bridges (Lys/Arg/N-terminus with ASP/GLU/C-

terminus) and hydrophobic (C-C) interactions and 3.5 Å for hydrogen bonds (polar-polar or charged-polar residue interactions). Total contact number values sum the contacts discovered in all three categories. Where interaction strengths are indicated, these values are computed using either:

$$\textbf{Polar interaction strength} = \sum_{sum}^{polar} \frac{1}{d} \quad (5)$$

where d is the distance between contacting residues for both salt bridge and h-bonds in the context of polar-type interactions (equation derived from calculations used to estimate the strength of electrostatic interactions[1]) or:

$$\textbf{Hydrophobic interaction strength} = \sum_{sum}^{hydrophobic} \frac{1}{d^6} \quad (6)$$

for apolar interaction strength values, where d is the distance between hydrophobic interacting amino acid residues (equation derived calculations used to estimate the strength of van der Waals interactions[1]). The final X-ray structure analysis method used here is computed using Equation 7:

$$\textbf{Monomer Proximity Index} = \frac{\sqrt{Size\ of\ Biological\ Dimer}}{Mon\text{-}Mon\ Distance} \quad (7)$$

where the larger the monomer proximity index value, the closer the packing of monomeric units within the dimer subcomplexes that comprise the tetramer.

PDB IDs for complexes studied here are: 1ICT for TTR, 3VHM for AVD, 1VAL for CON, 2HCY for ADH, 1ZAH for ALD, 1A5U for PKI, 4BLC for CAT and 1BGL for βGL.

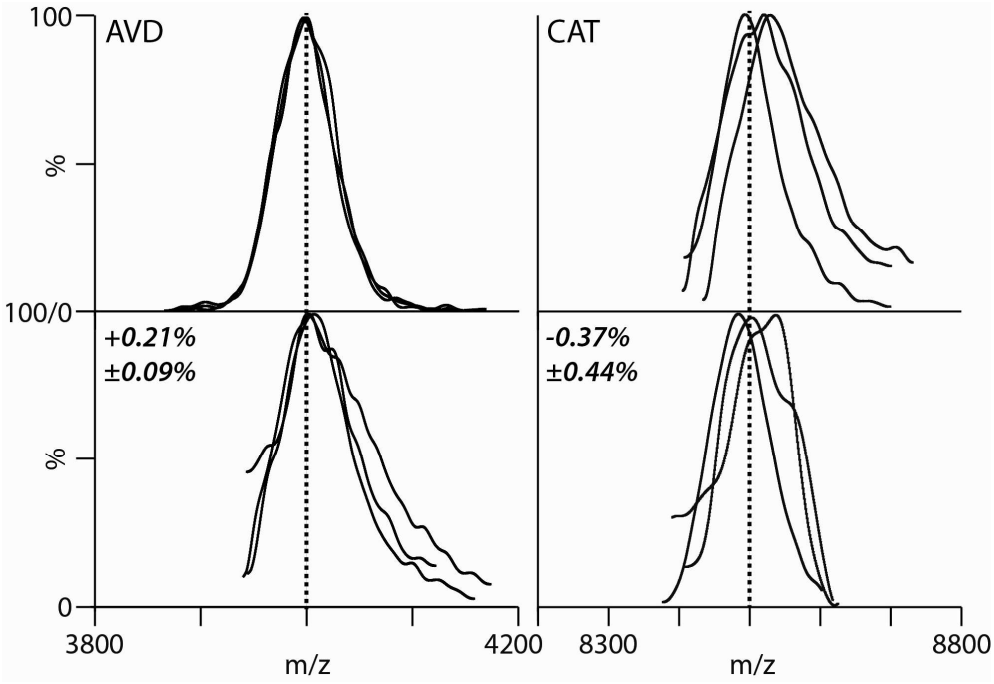

Figure S1. A comparison between the m/z and intact mass recorded for tetramer ions generated under control (200mM NH_4Ac, upper panel) and optimized disruption conditions (lower panel) discussed in Figure 3. Three replicates are measured and overlaid for each dataset shown. Minimum smoothing is used for the data shown. The charge states displayed are the 16^+ for AVD and the 28^+ for CAT. The actual mass shifts observed for these assemblies under conditions optimized for protein complex disruption were +8.7 Da for AVD and -31.9 Da for CAT, compared to control.

Table S1. Solution conditions optimized for protein complex disruption, used in Figure 3.

Protein complex	Solution Conditions Optimized for Protein Disruption
TTR	47% DMSO, 4M NH_4Ac
AVD	53% DMSO, 10mM NH_4Ac
CON	17% DMSO, 3M NH_4Ac
ADH	17% DMSO, 2M NH_4Ac
ALD	33% DMSO, 1M NH_4Ac
PKI	17% DMSO, 2M NH_4Ac
CAT	33% DMSO, 2M NH_4Ac
βGL	17% DMSO, 3M NH_4Ac

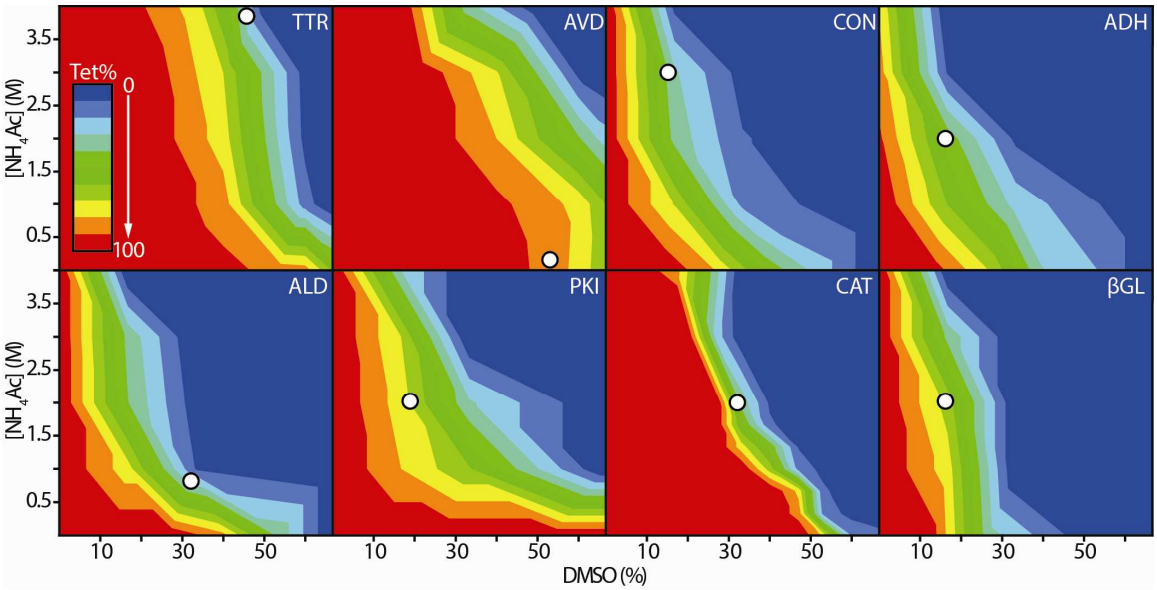

Figure S2. The positions of the disruption conditions shown in Table S1 within the 2D titration maps shown in Figure 5A. Conditions were selected based on two criteria: 1) That they contain optimized signal for both dimer and monomer ions and 2) that at least 50% of the intact tetramer had undergone dissociation. Conditions optimized for AVD disruption, as shown in Table S1 and discussed as the 'orange dataset' in Figure 4, were chosen to maximize dimer signal intensity, even though intact tetramer disruption is not as complete as in the other complexes studied here.

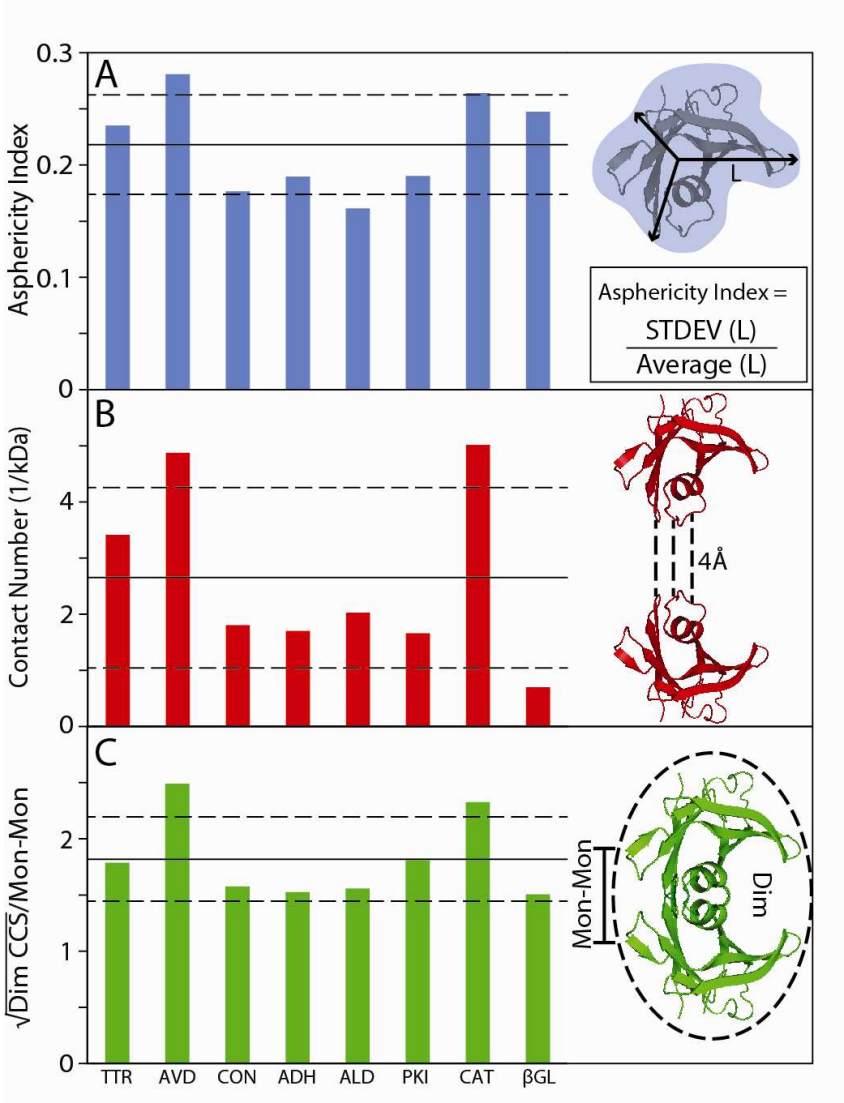

Figure S3. Comparing X-ray and IM-MS data provides critical insight into the structural deformations observed in AVD and CAT subcomplexes. (A) Asphericity index values calculated for subunits within each protein complex. Larger values indicate a less globular shape for protein subunits. (B) The average number of contacts per-unit kDa within the protein-protein interfaces of the complexes studied in this report. (C) A monomer proximity index, calculated using the square root of the dimer size divided by the linear distance between the monomers that form the biological dimer for each complex. The larger the index value, the more-tightly packed the monomers within the X-ray structure. For all panels, the solid lines shown indicate average values for each metric, while dashed lines indicate ± one standard deviation from the mean. Each value indicated is discussed in detail and defined in the text.

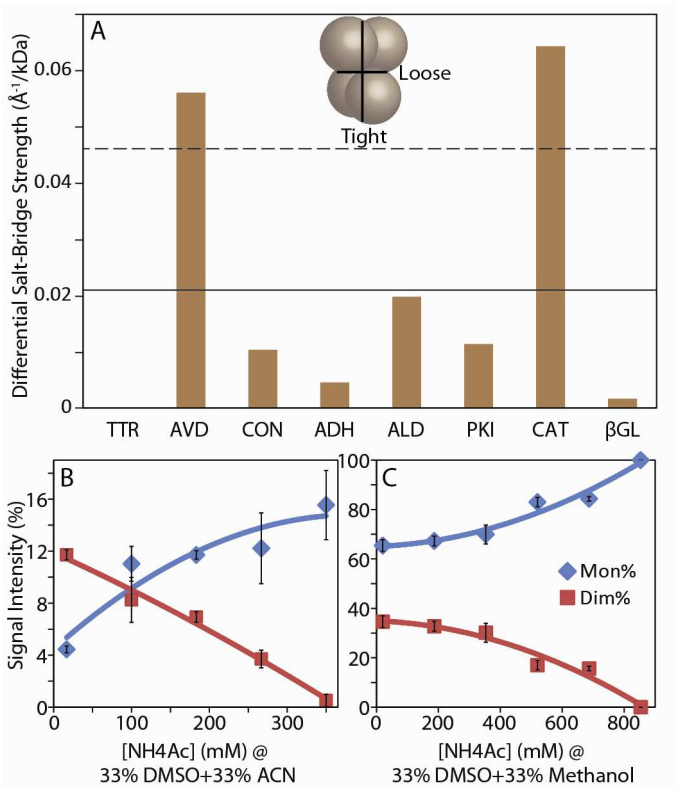

Figure S4. Correlations between IM-MS disruption experiments using a three-component titration strategy and salt bridge strength calculations from X-ray structure data (A) A histogram plot showing the calculated strength of the salt-bridge interactions found in the smaller 'loose' interfaces within the X-ray structures of the complexes studied here, over those found in the larger 'tight' interfaces. The solid line shown indicates the mean value for this ratio for all eight tetrameric proteins studied, while dashed line indicates + one standard deviation from the mean. An analysis of this ratio suggests that significant salt-bridge based interface strength asymmetry exists in the AVD and CAT tetramers, but not in the other complexes studied here. (B) Monomer and dimer intensity values recorded during the three-component disruption of the AVD tetramer, utilizing NH4Ac, DMSO and acetonitirle (ACN). Organic content in this plot is fixed at 33% DMSO and 33% ACN. (C) Monomer and dimer intensity values for the CAT tetramer using a similar screen as in B. Methanol replaces ACN, but total organic content is fixed 33% DMSO and 33% methanol. In both B and C, clear divergent trends are observed between monomer and dimer signal intensity, favoring dimer formation only at the low ionic strength values that favor the retention of inter-protein salt bridge formation.

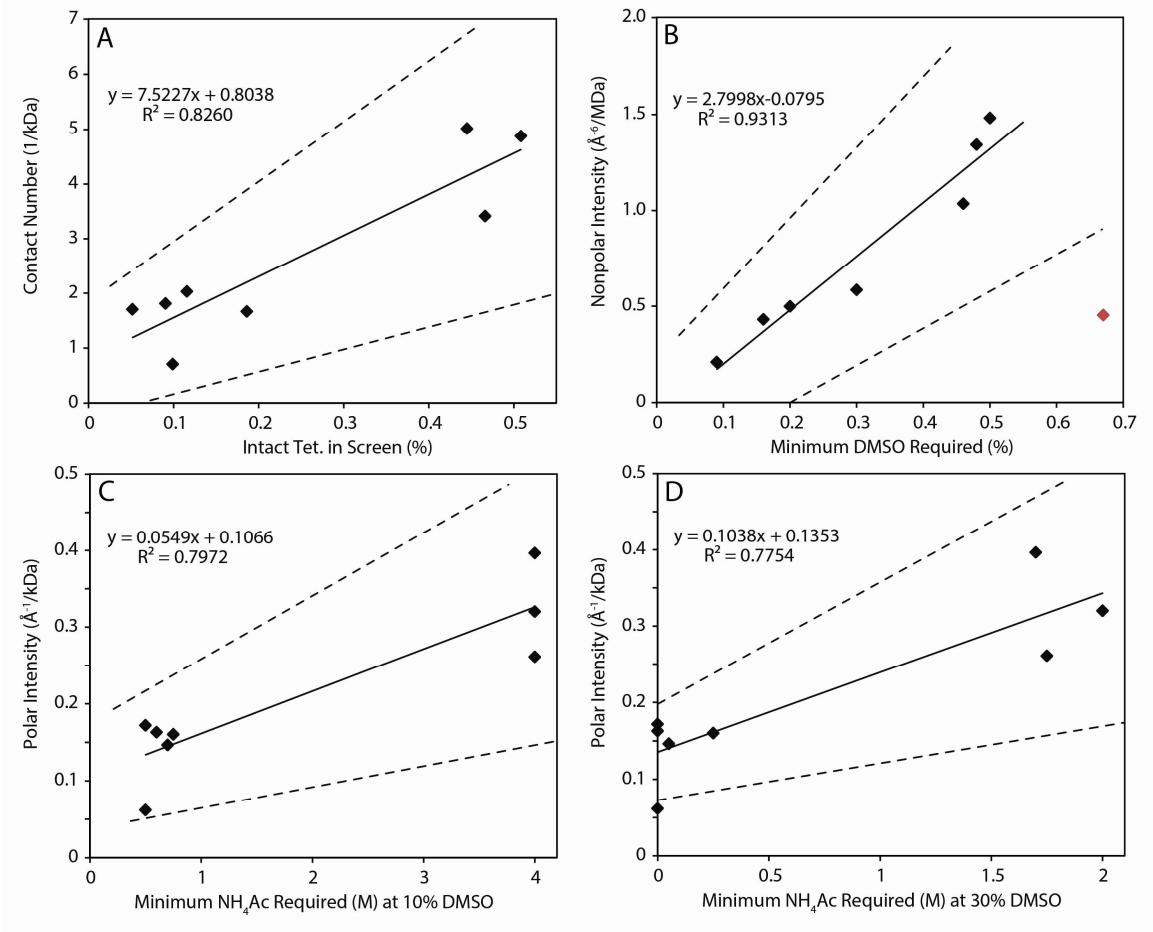

Figure S5. Correlations between our IM-MS titration experiments (X axis) and X-ray structure data (Y axis), shown as a scatter plot with fitted trend lines. Dashed lines indicate the 95% confidence interval for each fit. (A) Normalized intact tetramer intensity integrated over all disruption conditions vs. the number of contacts per unit kDa calculated from X-ray data. (B) The DMSO % in solution, without added NH_4Ac, required to initiate tetramer disruption (signal drops by 10%) vs. the estimated average strength of hydrophobic contacts within the protein-protein contacts from X-ray ($Å^{-6}$/MDa). Red data point represents PKI, which is excluded from the fit. (C) NH_4Ac concentration required for tetramer disruption at fixed 10% and 30% DMSO (D) vs. the estimated average strength of the polar interactions ($Å^{-1}$/kDa) within the protein-protein contacts from X-ray. The correlation equations and linear correlation coefficients between IM-MS and X-ray datasets are each shown in the corresponding panel. The error estimates in the text indicates the difference between calculated values from X-ray data and prediction values based on the linear correlations shown.

References

(1) Leach, A. R. *Molecular Modeling Principles and Applications; Prentice Hall*: Harlow, England, **2001**.